



# Well-Defined Strontium Tungstate Hierarchical Microspheres: Synthesis and Photoluminescence Properties

Guang Jia\*, Cuimiao Huang, Cuimiao Zhang, Shiwen Ding, and Liyong Wang

College of Chemistry and Environmental Science, Chemical Biology Key Laboratory of Hebei Province, Hebei University, Baoding 071002, P. R. China

Uniform and well-dispersed SrWO<sub>4</sub> microspheres have been successfully synthesized through a hydrothermal method by using trisodium citrate and SDS as surfactants. XRD and SEM results demonstrate that the as-synthesized SrWO<sub>4</sub> particles are high purity well crystallized and exhibit a relatively uniform spherical morphology. The as-obtained SrWO<sub>4</sub>:Ln<sup>3+</sup> (Ln = Tb, Eu, Dy, and Sm) microspheres show intense light emissions with different colors coming from different Ln<sup>3+</sup> ions under ultraviolet excitation, which might find potential applications in the fields such as light emitting phosphors, advanced flat panel displays, and light-emitting diodes (LEDs).

**Keywords:** Strontium Tungstate, Microspheres, Hydrothermal Synthesis, Luminescence Properties.

Delivered by Ingenta to: Nanyang Technological University  
IP: 91.198.127.81 On: Fri, 10 Jun 2016 14:07:28  
Copyright: American Scientific Publishers

## 1. INTRODUCTION

During the past decades, self-assembled micrometer-sized inorganic materials with special size, morphology, and hierarchy were of special interest in the areas of materials synthesis and device fabrication due to their hierarchical and repetitive structures, which show potential applications in wide fields of crystals, catalysis, diagnostics, and pharmacology.<sup>1–4</sup> In particular, three dimensional (3D) hierarchical particles have attracted special attention due to the practical importance related to some fractal growth process. Because the physicochemical properties of crystals depend not only on their chemical composition but also on the morphology and size, controllable synthesis of inorganic functional materials with high-ordered structures is very intriguing.<sup>5,6</sup> Many synthesis routes have been developed to fabricate the 3D inorganic hierarchical particles, such as sol–gel processes, precipitation, combustion, microemulsion, chemical vapor technique, and so forth. In these fabrications, the hydrothermal method, as a typical solution-based approach, has proved to be an effective and convenient synthesis technique for preparing various inorganic materials with diverse morphologies and architectures. Moreover, the complexing agents or surfactants always play an important role in controlling

the dynamics of crystal growth and determining the final morphology of the hierarchical nano-/microstructures during the hydrothermal process.

Recently, the scheelite-type structured tungstates with a general formula AWO<sub>4</sub> (A = Ca, Sr, Ba, Pb) have been extensively investigated due to their wide potential industrial applications such as scintillators,<sup>7</sup> phosphors,<sup>8–11</sup> batteries,<sup>12</sup> and solid-state lasers.<sup>13,14</sup> Among these metal tungstates, strontium tungstate (SrWO<sub>4</sub>) with typical scheelite-type is widely used in optoelectronic industry and solid state laser system due to its luminescence behavior and stimulating Raman scattering property.<sup>15</sup> In recent years, SrWO<sub>4</sub> which has been widely applied as eminent candidates for the matrix of lanthanide activator ions shows potential applications in optical displays and light-emitting diodes (LEDs).<sup>16–19</sup> To date, various morphologies of SrWO<sub>4</sub> have been prepared by different synthesis routes, such as nanoparticles,<sup>20</sup> nanobelts,<sup>21</sup> nanopeanuts and nanorods,<sup>22</sup> octahedron-like structure,<sup>23</sup> and thin films.<sup>15,24</sup> However, the synthesis of uniform and well-dispersed SrWO<sub>4</sub> microspheres has been rarely studied. On the other hand, it is well-established that the ideal morphology of phosphor particles includes a perfect spherical shape, narrow size distribution, and nonagglomeration. The spherical morphology phosphors is good for high brightness and high resolution because high packing densities and low scattering of light can be obtained by using

\* Author to whom correspondence should be addressed.

such phosphors.<sup>25,26</sup> So it is desirable to develop easily controllable methods for the synthesis of spherical SrWO<sub>4</sub> luminescent materials with promising novel luminescent properties.

In the present work, uniform and well-dispersed SrWO<sub>4</sub> hierarchical microspheres have been synthesized using a facile hydrothermal process in the presence of trisodium citrate and sodium dodecyl benzenesulfonate (SDS). Moreover, the luminescent properties of lanthanide activator ions Ln<sup>3+</sup> (Ln = Tb, Eu, Dy, and Sm) doped SrWO<sub>4</sub> samples, which may find potential applications in optical displays and light-emitting diodes, were investigated in detail.

## 2. EXPERIMENTAL DETAILS

### 2.1. Materials

Ln(NO<sub>3</sub>)<sub>3</sub> (Ln = Eu, Dy, and Sm) and Tb(NO<sub>3</sub>)<sub>3</sub> aqueous solutions were obtained by dissolving Ln<sub>2</sub>O<sub>3</sub> (99.99%) and Tb<sub>4</sub>O<sub>7</sub> (99.99%) in dilute HNO<sub>3</sub> solution under heating with agitation. All other chemicals were of analytical grade and used directly without further purification.

### 2.2. Preparation

In a typical synthesis, 2 mmol of Sr(Ac)<sub>2</sub> · 0.5 H<sub>2</sub>O (0.429 g) was first dissolved in 20 mL of deionized water. Meanwhile 2 mmol (0.588 g) of trisodium citrate (C<sub>6</sub>H<sub>5</sub>Na<sub>3</sub>O<sub>7</sub> · 2H<sub>2</sub>O) and 2 mmol (0.697 g) of sodium dodecyl benzenesulfonate (SDS, C<sub>18</sub>H<sub>29</sub>NaO<sub>3</sub>S) were added into the above solution under stirring. Subsequently, 4 mmol of Na<sub>2</sub>WO<sub>4</sub> solution (1.320 g of Na<sub>2</sub>WO<sub>4</sub> · 2H<sub>2</sub>O dissolved in 15 mL of deionized water) was slowly added to the above mixed solution. A well-controlled amount of HAc solution was then added with magnetic stirring to pH 5. After additional agitation for 10 min, the precursor solution was transferred into a Teflon-lined autoclave, sealed, and heated to 200 °C for 24 h. Then the autoclave was cooled to room temperature naturally. As the autoclave cooled to room temperature naturally, the precipitate was separated by centrifugation, washed with deionized water and ethanol in sequence, and then dried in air to obtain the final sample.

A similar process were employed to prepare Eu<sup>3+</sup>, Tb<sup>3+</sup>, Dy<sup>3+</sup>, and Sm<sup>3+</sup> doped SrWO<sub>4</sub> samples except for adding a stoichiometric amount (5 mol%) of Tb(NO<sub>3</sub>)<sub>3</sub>, Eu(NO<sub>3</sub>)<sub>3</sub>, Dy(NO<sub>3</sub>)<sub>3</sub>, and Sm(NO<sub>3</sub>)<sub>3</sub> aqueous solution instead of Sr(Ac)<sub>2</sub> at the initial stage [0.1 mmol of Ln(NO<sub>3</sub>)<sub>3</sub> solution (0.1 M, 1 mL; Ln = Tb, Eu, Dy, or Sm) was added into the Sr(Ac)<sub>2</sub> solution which contained 1.9 mmol of Sr(Ac)<sub>2</sub> · 0.5 H<sub>2</sub>O (0.408 g)]. For comparison, the experiment was performed to prepare SrWO<sub>4</sub> sample via a similar process by solely adding trisodium citrate or SDS as surfactant.

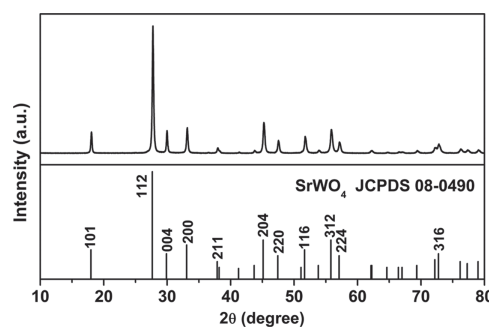


**Fig. 1.** XRD pattern of SrWO<sub>4</sub> sample prepared with trisodium citrate and SDS as surfactants. The standard data of tetragonal SrWO<sub>4</sub> (JCPDS No. 08-0490) is presented as a reference.

### 2.3. Characterization

The samples were characterized by powder X-ray diffraction (XRD) performed on a D8 Advance diffractometer (Bruker). Fourier transform infrared spectroscopy (FT-IR) spectra were measured with a Perkin-Elmer 580B infrared spectrophotometer. The morphology and composition of the samples were inspected using JSM-7500F cold field scanning electron microscope JEOL equipped with an energy-dispersive X-ray spectrum. Photoluminescence (PL) excitation and emission spectra were recorded with a Hitachi F-4500 spectrophotometer. All measurements were performed at room temperature.

## 3. RESULTS AND DISCUSSION

Figure 1 shows the XRD pattern of the SrWO<sub>4</sub> sample prepared at 200 °C for 24 h with trisodium citrate and SDS as surfactants. From Figure 1, one can see that the diffraction peaks agree well with the reported data of scheelite structure SrWO<sub>4</sub> with tetragonal phase [JCPDS Card No. 08-0490, Space group: I41/a (88)]. No other additional peaks can be detected, indicating that the simple hydrothermal method is a feasible route to prepare pure phase of SrWO<sub>4</sub>. It should be mentioned that the diffraction peaks of SrWO<sub>4</sub>:Ln<sup>3+</sup> (Ln = Eu, Tb, Dy, and Sm) samples can also agree well with tetragonal scheelite-type SrWO<sub>4</sub>, indicating that the Ln<sup>3+</sup> ions have been effectively doped into the SrWO<sub>4</sub> host lattice. Moreover, the XRD patterns of the samples prepared by solely adding trisodium citrate or SDS also coincide with scheelite-type SrWO<sub>4</sub> (not shown). Moreover, it can also be seen that the diffraction peaks of the SrWO<sub>4</sub> sample are very strong and sharp, so we can say this product has high crystallinity. It is joyous, because when the phosphor has high crystallinity it may has less traps and exhibit stronger luminescence.

The energy dispersive X-ray (EDX) spectrum was further used to investigate the as-obtained SrWO<sub>4</sub> sample (Fig. 2). The EDX spectrum of the sample confirms the presence of strontium (Sr), tungstate (W), and oxygen (O)

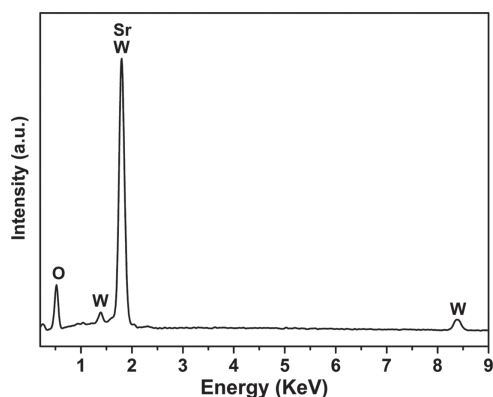


Fig. 2. EDX spectrum of the as-obtained  $\text{SrWO}_4$  sample.

elements. No other impurity peaks can be detected, which can effectively support the XRD result of the sample.

Figure 3 shows the FT-IR spectrum of as-synthesized  $\text{SrWO}_4$  sample. The absorption bands at  $3423\text{ cm}^{-1}$  and  $1622\text{ cm}^{-1}$  are assigned to O—H stretching vibration and H—O—H bending vibration,<sup>27,28</sup> which are the characteristic vibrations of water absorbed on the surface of  $\text{SrWO}_4$  sample. A small band at  $1406\text{ cm}^{-1}$  is characteristic of the symmetrical vibrations of the carboxylate groups, which proved the citric ions capping on  $\text{SrWO}_4$  sample. The absorption band centered at  $2367\text{ cm}^{-1}$  is attributed to the atmospheric absorbed  $\text{CO}_2$  on the surface of  $\text{SrWO}_4$  sample. The sharp band at  $808\text{ cm}^{-1}$  is due to the O—W—O stretches of the  $\text{WO}_4$  tetrahedron, and the band at  $442\text{ cm}^{-1}$  is assigned to the Au mode of  $\text{WO}_4^{2-}$ .<sup>20,28,29</sup> The result agrees well with the XRD and EDX analysis, which provides additional evidence for the formation of the  $\text{SrWO}_4$  product.

The SEM and TEM images were used to characterize the morphology of as-prepared  $\text{SrWO}_4$  samples. It should be mentioned that doping a small amount of lanthanide ions ( $\text{Tb}^{3+}$ ,  $\text{Eu}^{3+}$ ,  $\text{Dy}^{3+}$ , and  $\text{Sm}^{3+}$ ) in the  $\text{SrWO}_4$  host does not change the crystal phase and morphology of the  $\text{SrWO}_4$  products in our present work. So here we only

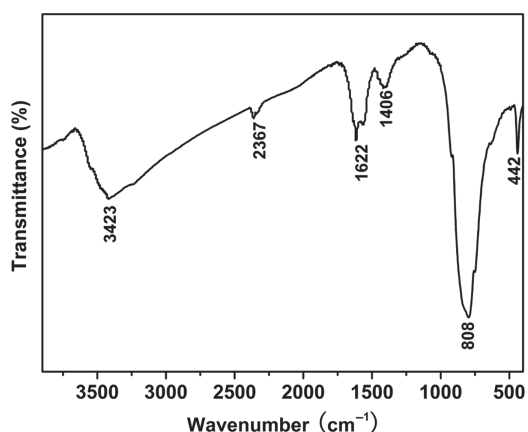


Fig. 3. FT-IR spectrum of  $\text{SrWO}_4$  sample.

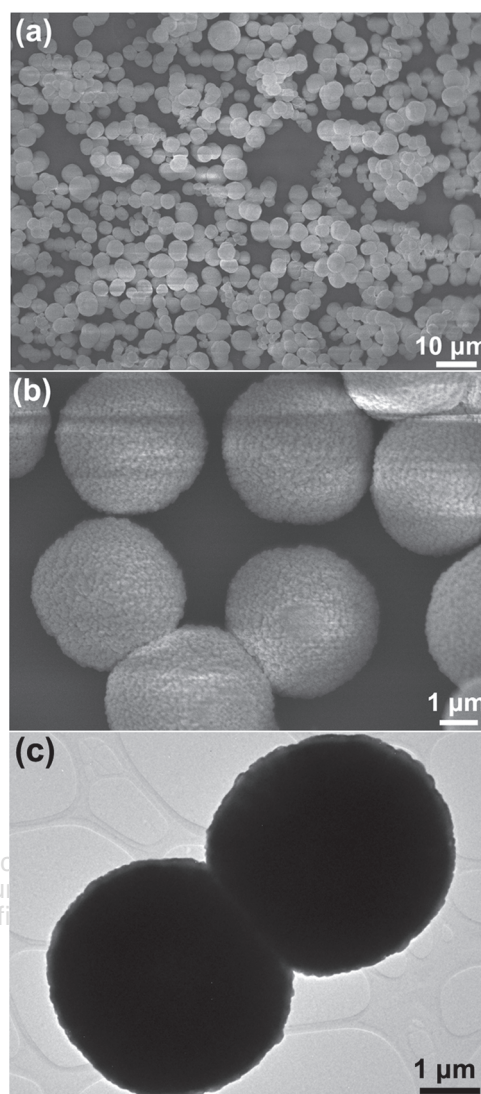
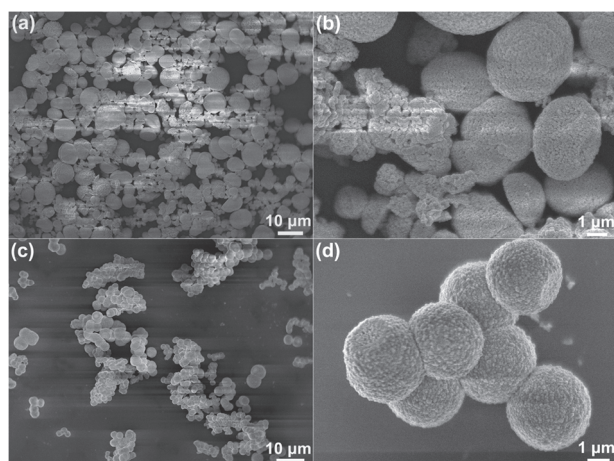


Fig. 4. (a), (b) SEM and (c) TEM images of the  $\text{SrWO}_4$  sample prepared with trisodium citrate and SDS as surfactants.

take pure  $\text{SrWO}_4$  sample as an example to illustrate the morphology of the products. From the low-magnification SEM images of the  $\text{SrWO}_4$  sample with trisodium citrate and SDS as surfactants, it can be seen that the as-obtained  $\text{SrWO}_4$  sample consists of a large scale of uniform and well-dispersed microspheres (Fig. 4(a)). The diameters of the microspheres are about  $4\text{ }\mu\text{m}$ . From the enlarged SEM image, one can observe that the surface of the hierarchical microsphere is not smooth and an individual sphere is not a single particle but the assembly of tiny packed nanocrystallites (Fig. 4(b)). To provide further insight into the  $\text{SrWO}_4$  composite particles, TEM investigation was also performed (Fig. 4(c)). The TEM images of the  $\text{SrWO}_4$  sample exhibit the spherical morphology with good dispersion and the diameters of the microspheres are about  $4\text{ }\mu\text{m}$ , which agrees well with the SEM images. The perfect



**Fig. 5.** SEM images of the  $\text{SrWO}_4$  samples prepared with (a), (b) trisodium citrate or (c), (d) SDS as surfactant.

spherical phosphor particles may have potential to be an excellent host material for luminescent materials.<sup>25,26</sup>

In order to identify the influence of the surfactants, the  $\text{SrWO}_4$  samples were prepared by solely adding trisodium citrate or SDS as surfactant during the hydrothermal process. Figures 5(a), (b) shows the SEM images of  $\text{SrWO}_4$  sample prepared with trisodium citrate as surfactant. It can be seen that the sample consist of microspheres and irregular particles with broad size distribution. The  $\text{SrWO}_4$  sample prepared with SDS as surfactant is mainly composed of microspheres with diameters of about  $3.5 \mu\text{m}$ , but the sample becomes badly-dispersed in distribution due to the aggregation of microspheres (Figs. 5(c), (d)). On the basis of the results mentioned above, it is presumed that the trisodium citrate and SDS may exhibit a synergistic effect in controlling the crystal growth and self-assembly of  $\text{SrWO}_4$  sample during the hydrothermal process, resulting in the uniform and well-dispersed  $\text{SrWO}_4$  microspheres.

The photoluminescence (PL) properties of the as-synthesized  $\text{SrWO}_4:\text{Ln}^{3+}$  ( $\text{Ln} = \text{Tb}, \text{Eu}, \text{Dy}, \text{and Sm}$ ) samples were characterized by the PL excitation and emission spectra (Figs. 6, 7). The excitation spectra of  $\text{SrWO}_4:\text{Tb}^{3+}$  sample consist of a broad band centered at 250 nm and some weak peaks between 300 and 500 nm (Fig. 6(a)), which are ascribed to the transition from the  $^1\text{A}_1$  ground-state to the high vibration level of  $^1\text{T}_2$  within the  $\text{WO}_4^{2-}$  group and  $f-f$  transitions of  $\text{Tb}^{3+}$  ions.<sup>19</sup> The absorption intensity of the  $\text{Tb}^{3+}$   $f-f$  transitions is very weak in comparison with that of the  $\text{WO}_4^{2-}$  group, indicating that the excitation of the  $\text{Tb}^{3+}$  ions is mainly through the energy transfer from the  $\text{WO}_4^{2-}$  group to  $\text{Tb}^{3+}$  ions. Upon excitation into the  $\text{WO}_4^{2-}$  group at 250 nm, one can see that  $\text{SrWO}_4:\text{Tb}^{3+}$  sample shows the most intense emission peak corresponding to the green  $^5\text{D}_4-^7\text{F}_5$  hypersensitive transition of  $\text{Tb}^{3+}$  located at 544 nm. Three other peaks are observed at 491, 589, and 624 nm, which correspond to the

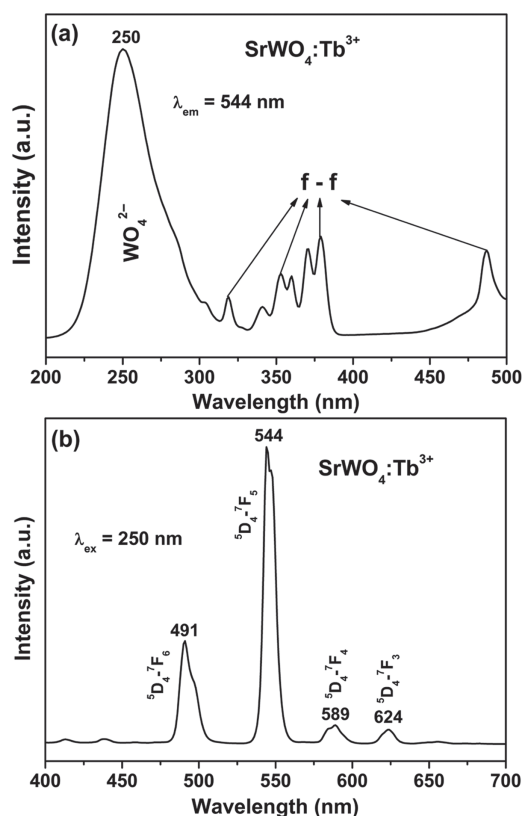


**Fig. 6.** Photoluminescence (a) excitation and (b) emission spectra of  $\text{SrWO}_4:\text{Tb}^{3+}$  sample.

$^5\text{D}_4-^7\text{F}_6$ ,  $^5\text{D}_4-^7\text{F}_4$ , and  $^5\text{D}_4-^7\text{F}_3$  transitions of  $\text{Tb}^{3+}$  ions, respectively (Fig. 6(b)). From the emission spectra, it can be seen that no emission from the  $\text{WO}_4^{2-}$  group is observed, suggesting that the energy transfer from  $\text{WO}_4^{2-}$  to  $\text{Tb}^{3+}$  is very efficient.

The excitation spectrum of  $\text{SrWO}_4:\text{Eu}^{3+}$  sample consists of a broad band with a maximum at about 281 nm and some sharp peaks between 350 and 500 nm (Fig. 7(a)). The broad band at 281 nm can be assigned to the charge transfer state from the excited 2p orbits of  $\text{O}^{2-}$  to the empty orbits of the central  $\text{W}^{6+}$  of the  $\text{WO}_4^{2-}$  groups. The dominant sharp peaks at 394 and 464 nm can be attributed to the  $^7\text{F}_0-^5\text{L}_6$  and  $^7\text{F}_0-^5\text{D}_2$  transitions within the  $4f^6$  configuration of  $\text{Eu}^{3+}$  ions, respectively.<sup>30</sup> Upon excitation at 394 nm, the emission spectrum of  $\text{SrWO}_4:\text{Eu}^{3+}$  sample is composed of a group of lines at about 593, 617, 656, and 703 nm (Fig. 7(b)), which can be attributed to  $^5\text{D}_0-^7\text{F}_j$  ( $J = 1, 2, 3, 4$ ) transition lines of the  $\text{Eu}^{3+}$  ions, respectively. The emission spectra are dominated by the  $^5\text{D}_0-^7\text{F}_2$  (617 nm) transition of  $\text{Eu}^{3+}$ , which is an electric-dipole allowed transition and hypersensitive to the environment. The excitation spectra of  $\text{SrWO}_4:\text{Dy}^{3+}$  and  $\text{SrWO}_4:\text{Sm}^{3+}$  samples also consist of a broad band of  $\text{WO}_4^{2-}$  groups and the  $f-f$  transitions of  $\text{Dy}^{3+}$  and  $\text{Sm}^{3+}$  ions, which are similar to that of  $\text{SrWO}_4:\text{Eu}^{3+}$  sample (not shown). The emission spectrum of  $\text{SrWO}_4:\text{Dy}^{3+}$  sample consists of

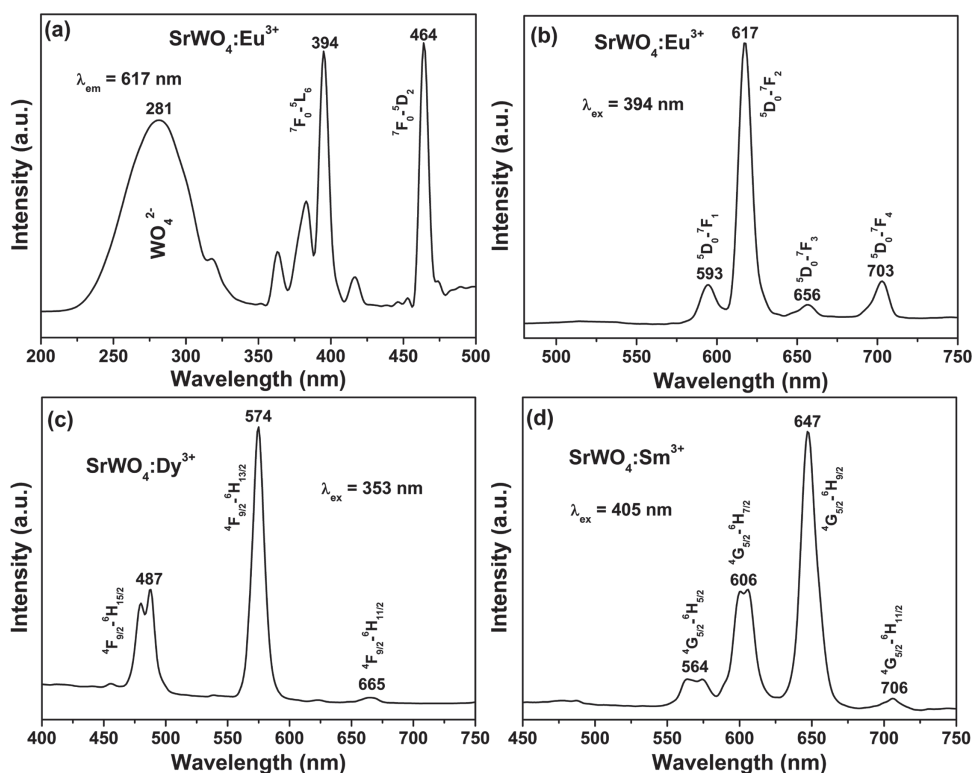


Fig. 7. (a) Excitation and (b) emission spectra of  $\text{SrWO}_4:\text{Eu}^{3+}$  sample and emission spectra of (c)  $\text{SrWO}_4:\text{Dy}^{3+}$  and (d)  $\text{SrWO}_4:\text{Sm}^{3+}$  samples.

three emission lines at 487, 574, and 665 nm, which are assigned to the  ${}^4\text{F}_{9/2}-{}^6\text{H}_{15/2}$ ,  ${}^4\text{F}_{9/2}-{}^6\text{H}_{13/2}$ , and  ${}^4\text{F}_{9/2}-{}^6\text{H}_{11/2}$  transition lines of  $\text{Dy}^{3+}$  ions (Fig. 7(c)), respectively. The  $\text{SrWO}_4:\text{Sm}^{3+}$  sample exhibits the characteristic emission lines of  $\text{Sm}^{3+}$  at 564, 606, 647, and 706 nm, which

corresponds to the  ${}^4\text{G}_{5/2}-{}^6\text{H}_J$  ( $J = 5/2, 7/2, 9/2, 11/2$ ) transition of  $\text{Sm}^{3+}$  ions (Fig. 7(d)). The result agrees well with the previous literatures.<sup>31,32</sup>

The  $\text{SrWO}_4:\text{Ln}^{3+}$  ( $\text{Ln} = \text{Tb}, \text{Eu}, \text{Dy}, \text{and Sm}$ ) samples exhibit strong green, red, yellow, and orange-red emissions under ultraviolet excitation, which can be confirmed by the CIE (Commission Internationale de l'Éclairage 1931 chromaticity) coordinates for the emission spectra of the  $\text{SrWO}_4:\text{Ln}^{3+}$  samples (Fig. 8). The chromaticity coordinates of  $\text{SrWO}_4:\text{Ln}^{3+}$  ( $\text{Ln} = \text{Tb}, \text{Eu}, \text{Dy}, \text{and Sm}$ ) samples are calculated to be  $x = 0.251, y = 0.602$ ;  $x = 0.606, y = 0.338$ ;  $x = 0.429, y = 0.442$ ; and  $x = 0.511, y = 0.356$ , located in the green, red, yellow, and orange-red region, respectively. On the basis of the above results, it can be concluded that the PL emission colors of the uniform  $\text{SrWO}_4:\text{Ln}^{3+}$  microspheres can be tuned from green to yellow to red by doping different lanthanide activator ions.

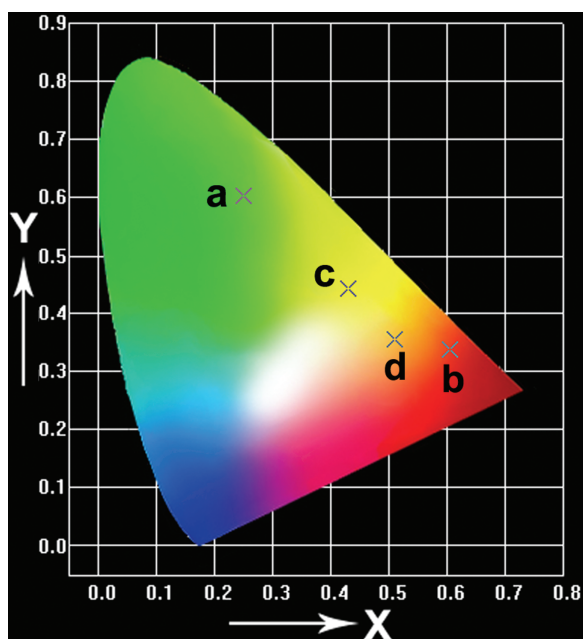


Fig. 8. CIE chromaticity diagram of  $\text{SrWO}_4:\text{Ln}^{3+}$  samples: (a)  $\text{Tb}^{3+}$ , (b)  $\text{Eu}^{3+}$ , (c)  $\text{Dy}^{3+}$ , and (d)  $\text{Sm}^{3+}$ .

potentially applied in optical displays and light-emitting diodes (LEDs). Furthermore, this general and facile method may be of much significance in the synthesis of other tungsten functional materials.

**Acknowledgments:** This work is financially supported by the Natural Science Foundation of Hebei Province (Grant No. B2012201074), University Scientific Research Project (Grant No. 2011171) and Outstanding Youth Fund Project (Grant No. Y2012007) of Hebei Education Department, and Research Plans of the Natural Science Foundations (Grant Nos. 2010–200, 2012–234) and Laboratory Open Foundations (Grant Nos. 2012015, 2012025) of Hebei University.

## References and Notes

1. C. Burda, X. Chen, R. Narayanan, and M. A. El-Sayed, *Chem. Rev.* 105, 1025 (2005).
2. Z. W. Pan, Z. R. Dai, and Z. L. Wang, *Science* 291, 1947 (2001).
3. W. Scharfl, *Adv. Mater.* 12, 1899 (2000).
4. F. Caruso, *Adv. Mater.* 13, 11 (2001).
5. G. Jia, C. Zhang, S. Ding, and L. Wang, *J. Nanosci. Nanotechnol.* 11, 6875 (2011).
6. P. Yang, C. Li, W. Wang, Z. Quan, S. Gai, and J. Lin, *J. Solid State Chem.* 182, 2510 (2009).
7. D. Errandonea, D. Martinez-Garcia, R. Lacombe-Perales, J. Ruiz-Fuertes, and A. Segura, *Appl. Phys. Lett.* 89, 091913 (2006).
8. Z. Y. Zhou, C. X. Li, J. Yang, H. Z. Lian, P. P. Yang, R. T. Chai, Z. Y. Cheng, and J. Lin, *J. Mater. Chem.* 19, 2737 (2009).
9. R. P. Jia, G. X. Zhang, Q. S. Wu, and Y. P. Ding, *Appl. Phys. Lett.* 89, 043112 (2006).
10. Y. G. Su, L. P. Li, and G. S. Li, *Chem. Mater.* 20, 6060 (2008).
11. Y. G. Su, L. P. Li, and G. S. Li, *Chem. Commun.* 4004 (2008).
12. A. Kudo, M. Steinberg, A. J. Bard, A. Campion, M. A. Fox, T. E. Mallouk, S. E. Webber, and J. M. White, *Catal. Lett.* 5, 61 (1990).
13. J. Sulc, H. Jelinkova, T. T. Basiev, M. E. Doroschenko, L. I. Ivleva, V. V. Osiko, and P. G. Zverev, *Opt. Mater.* 30, 195 (2007).
14. Z. H. Cong, X. Y. Zhang, Q. P. Wang, Z. J. Liu, S. T. Li, X. H. Chen, X. L. Zhang, S. Z. Fan, H. J. Zhang, and X. T. Tao, *Opt. Lett.* 34, 2610 (2009).
15. Z. Lou and M. Cocivera, *Mater. Res. Bull.* 37, 1573 (2002).
16. Z. H. Ju, R. P. Wei, J. X. Ma, C. R. Pang, and W. S. Liu, *J. Alloys Compd.* 507, 133 (2010).
17. J. Liao, L. Liu, Ha. You, H. Huang, and W. You, *Optik* 123, 901 (2012).
18. J. Liao, B. Qiu, H. Wen, J. Chen, W. You, and L. Liu, *J. Alloys Compd.* 487, 758 (2009).
19. J. Liao, B. Qiu, H. Wen, J. Chen, and W. You, *Mater. Res. Bull.* 44, 1863 (2009).
20. T. Thongtem, S. Kungwankunakorn, B. Kuntalue, A. Phuruangrat, and S. Thongtem, *J. Alloys Compd.* 506, 475 (2010).
21. L. D. Feng, X. B. Chen, and C. J. Mao, *Mater. Lett.* 64, 2420 (2010).
22. L. Sun, Q. Guo, X. Wu, S. Luo, W. Pan, K. Huang, J. Lu, L. Ren, M. Cao, and C. Hu, *J. Phys. Chem. C* 111, 532 (2007).
23. J. C. Sczancoski, L. S. Cavalcante, M. R. Joya, J. W. M. Espinosa, P. S. Pizani, J. A. Varela, and E. Longo, *J. Colloid Interf. Sci.* 330, 227 (2009).
24. C. Cui, Ji. Bi, and D. Gao, *J. Cryst. Growth* 310, 4385 (2008).
25. J. Lin, M. Yu, C. Lin, and X. Liu, *J. Phys. Chem. C* 111, 5835 (2007).
26. J. Yang, Z. Quan, D. Kong, X. Liu, and J. Lin, *Cryst. Growth Des.* 7, 730 (2007).
27. A. Kato, S. Oishi, T. Shishido, M. Yamazaki, and S. Iida, *J. Phys. Chem. Solids* 66, 2079 (2005).
28. F. Lei and B. Yan, *J. Solid State Chem.* 181, 855 (2008).
29. S. P. S. Porto and J. F. Scott, *Phys. Rev.* 157, 716 (1967).
30. C. A. Kodaira, H. F. Brito, and M. C. F. C. Felinto, *J. Solid State Chem.* 171, 401 (2003).
31. X. Wu, J. Du, H. Li, M. Zhang, B. Xi, H. Fan, Y. Zhu, and Y. Qian, *J. Solid State Chem.* 180, 3288 (2007).
32. E. K. Ryu and Y. D. Huh, *Bull. Korean Chem. Soc.* 29, 503 (2008).

Received: 17 May 2012. Accepted: 29 September 2012.